DOI: 10.1002/cmdc.200600171

Topical Delivery of Silver Nanoparticles Promotes Wound Healing

Jun Tian,[a] Kenneth K. Y. Wong,*[a] Chi-Ming Ho,[b] Chun-Nam Lok,[c] Wing-Yiu Yu,[b] Chi-Ming Che,[b] Jen-Fu Chiu,[c] and Paul K. H. Tam[a]

Wound healing is a complex process and has been the subject of intense research for a long time. The recent emergence of nanotechnology has provided a new therapeutic modality in silver nanoparticles for use in burn wounds. Nonetheless, the beneficial effects of silver nanoparticles on wound healing remain unknown. We investigated the wound-healing properties of silver nanoparticles in an animal model and found that rapid healing and improved cosmetic appearance occur in a dose-dependent manner. Furthermore, through quantitative PCR, immunohistochemistry, and proteomic studies, we showed that silver nanoparticles exert positive effects through their antimicrobial properties, reduction in wound inflammation, and modulation of fibrogenic cytokines. These results have given insight into the actions of silver and have provided a novel therapeutic direction for wound treatment in clinical practice.

Introduction

The ultimate goal for wound healing is a speedy recovery with minimal scarring and maximal function. Wound healing proceeds through an overlapping pattern of events including coagulation, inflammation, proliferation, and matrix and tissue remodeling. For this efficient and highly controlled repair process to take place, numerous cell-signaling events are required. Although cytokines are crucial in initiating, sustaining, and regulating the post-injury response, these same molecules have been implicated in impaired wound healing, abnormal scar formation, and uncontrolled inflammatory response.[1–3] In terms of impaired wound healing, enhanced expression of TGF-β mRNA has been found in both keloids and hypertrophic scars.[4,5] In contrast, a lack of TGF-β has been demonstrated to result in scarless healing in a fetal wound model.[6] Indeed, inhibitors of TGF-β have been shown to reduce inflammation and scarring.[7,8] Cumulatively, these results suggest that TGF-β plays an important role in tissue fibrosis and post-injury scarring.

Furthermore, the pro-inflammatory cytokine IL-6 has been shown to be a potent stimulator of fibroblast proliferation.[9] IL-6 production is diminished in fetal wounds, whereas the exogenous administration of IL-6 to these wounds has been shown to lead to scarring. Thus the diminished pro-inflammatory cytokine response observed in fetal wounds may explain the scarless wound healing observed in utero, and this provides evidence that IL-6 may also be involved in scar formation in adults.[10]

Interferon-γ (IFN-γ) production by T lymphocytes and macrophages plays an important role in the tissue remodeling of wounds. The reduction of wound contraction by IFN-γ is mediated by retarding collagen production and lattice cross-linking with an increase in collagenase production.[11–13] These properties have stimulated much attention in IFN-γ therapy for the treatment of hypertrophic and keloid scars.[14]

For interleukin-10 (IL-10), when neutralizing antibodies were applied to incisional wounds, an increase in the infiltration of neutrophils and macrophages was observed as well as an increase in the expression of chemokines and proinflammatory cytokines.[15] Furthermore, in a fetal scarless healing model, wounded IL-10-null grafts were characterized by a significantly higher inflammatory cell infiltration and collagen deposition and an adult-like scarring response.[16] These results suggest the important role of IL-10 in regulating the expression of proinflammatory cytokines in wounds, leading to decreased matrix deposition and scar-free healing. Taken all the evidence thus far together, it would appear that inflammation is intimately linked to wound healing in normal circumstance. Nonetheless, in a wound-healing model in PU.1-null mice, which are genetically incapable of raising the standard inflammatory response owing to a lack of macrophages and neutrophils, it was shown that the repair of skin wounds took place in a scar-free manner.[17,18] This suggests that inflammation may be detrimental to the wound-healing process.

[a] *Dr. J. Tian, Dr. K. K. Y. Wong, Prof. P. K. H. Tam*
Department of Surgery, Li Ka Shing Faculty of Medicine
University of Hong Kong, Queen Mary Hospital, Hong Kong SAR (China)
Fax: (+852) 2817-3155
E-mail: kkywong@hkucc.hku.hk

[b] *Dr. C.-M. Ho, Dr. W.-Y. Yu, Prof. C.-M. Che*
Department of Chemistry, University of Hong Kong, Hong Kong SAR (China)

[c] *Dr. C.-N. Lok, Prof. J.-F. Chiu*
Department of Anatomy, Li Ka Shing Faculty of Medicine
University of Hong Kong, Hong Kong SAR (China)

Silver has been used for centuries to prevent and treat a variety of diseases including pleurodesis, cauterisation, and healing of skin wounds.[19–21] Its antibacterial effect may be due to blockage of the respiratory enzyme pathways and alteration of microbial DNA and the cell wall.[22] In addition to its recognized antibacterial properties, some authors have reported on the possible pro-healing properties of silver.[23] The use of silver in the past has been restrained by the need to produce silver as a compound, thereby increasing the potential side effects. Nanotechnology has provided a way of producing pure silver nanoparticles. This system also markedly increases the rate of silver ion release.[24] Recently, we demonstrated that silver nanoparticles exhibit cytoprotective activities toward HIV-1-infected cells.[25] Published studies of silver nanoparticles on wound healing are sparse, and the mechanism of action remains unknown. Herein we report that silver nanoparticles can promote wound healing and reduce scar appearance in a dose-dependent manner. Furthermore, our studies show that silver nanoparticles act by decreasing inflammation through cytokine modulation. The potential benefits of silver nanoparticles in all wounds can therefore be enormous.

Results

Silver nanoparticles promote healing and achieve better cosmesis

In our thermal injury model, the deep partial-thickness wounds normally healed after 35.4 ± 1.29 days (mean $\pm$SE). In animals treated with silver nanoparticles (ND), these healed in 26.5 ± 0.93 days, whereas wounds treated with silver sulfadiazine (SSD) needed 37.4 ± 3.43 days ($p < 0.01$) (Figure 1 A). The rate of healing in the three groups was also compared. As with healing time, rate of healing was increased in animals treated with ND ($p < 0.01$) (Figure 1 B). These observations indicate that wound healing is accelerated by silver nanoparticles.

We next compared the appearance of healed wounds. We found that wounds in the ND group showed the most resemblance to normal skin, with less hypertrophic scarring and nearly normal hair growth on the wound surface. The worst cosmetic appearance was observed in the SSD treatment group (Figure 1 C). Under histological evaluation, healed wounds from the ND group resembled normal skin, with a thin

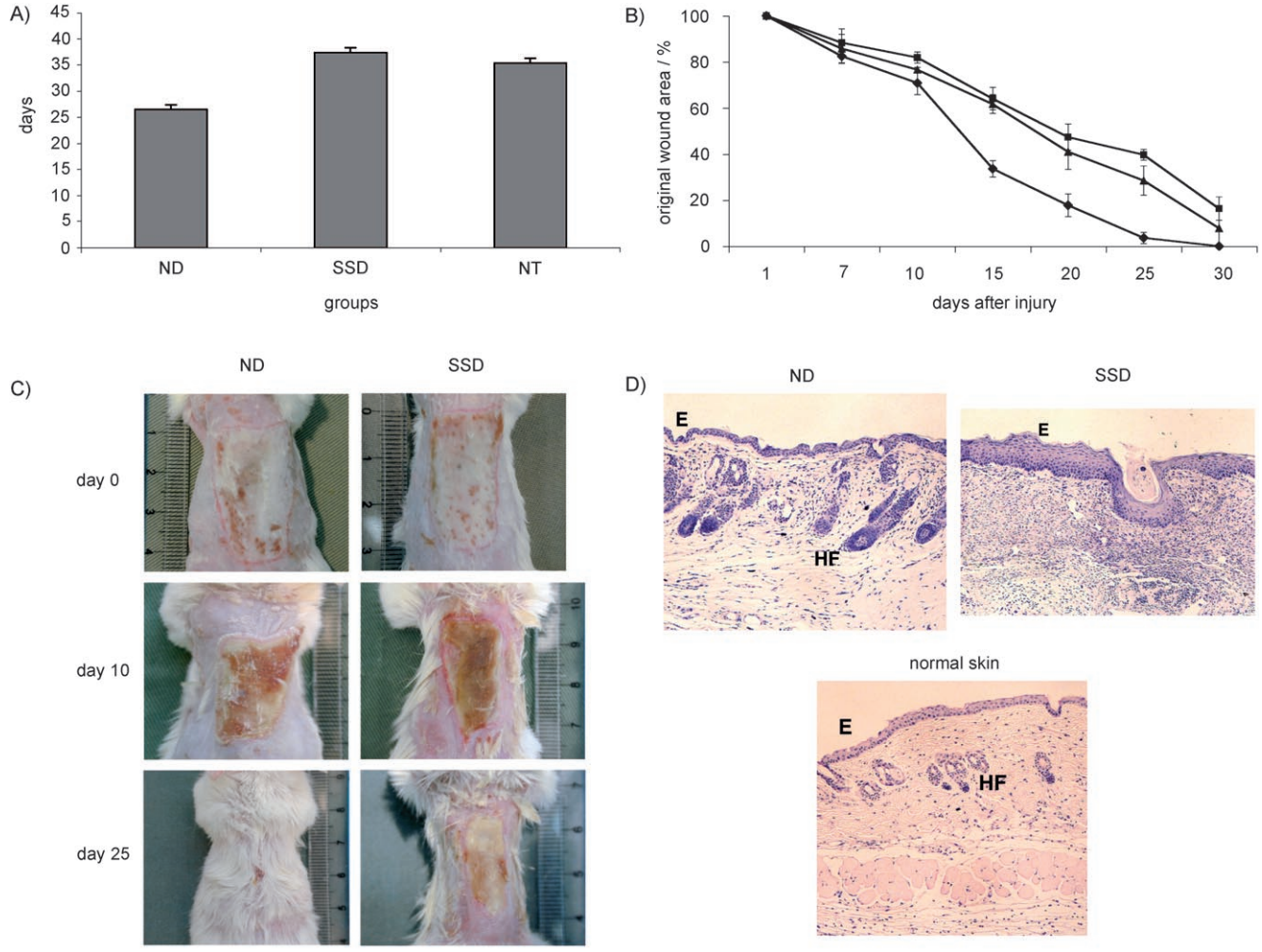

Figure 1. Silver nanoparticles accelerate wound healing and achieve superior cosmetic outcome: A) Time taken for burn wounds to heal in animals treated with silver nanoparticles (ND), silver sulfadiazine (SSD), and no treatment (NT). B) The rate of wound healing in burn animals treated with ND (◆), SSD (■), or no treatment (▲). C) Photographs of wounds from animals treated with ND, SSD, or no treatment on days 0, 10, and 25 after burn injury. D) Hematoxylin and eosin staining of histological sections of healed wounds from animals treated with ND, SSD, or no treatment (E = epidermis, HF = hair follicle; 40× mag.).

epidermis and nearly normal hair follicles. In contrast, histological sections from the SSD-treated group showed thickened epidermis and no evidence of hair growth (Figure 1 D).

Silver nanoparticles have effective antibacterial properties

As silver is known to be an effective antibacterial agent, we next determined whether the observed effect of silver nanoparticles is due solely to their antimicrobial property. We first compared the effect of ND toward bacterial colonization on wounds after thermal injury. Wound culture showed no microorganism growth up to 7 days after injury in the ND group. In contrast, bacterial growth was found in the SSD group 3 days after injury. This confirmed that silver nanoparticles are a more effective antibacterial agent (Figure 2 A). With this in mind, we then compared ND with amoxicillin and metronidazole, two commonly used antibiotics. Wounds treated with ND completely healed in 25.2 ± 0.72 days after injury, whereas those treated with antibiotics required 28.6 ± 1.02 days ($p < 0.01$) (Figure 2 B). This finding suggests that other factors are also involved in the mechanism of action of silver nanoparticles.

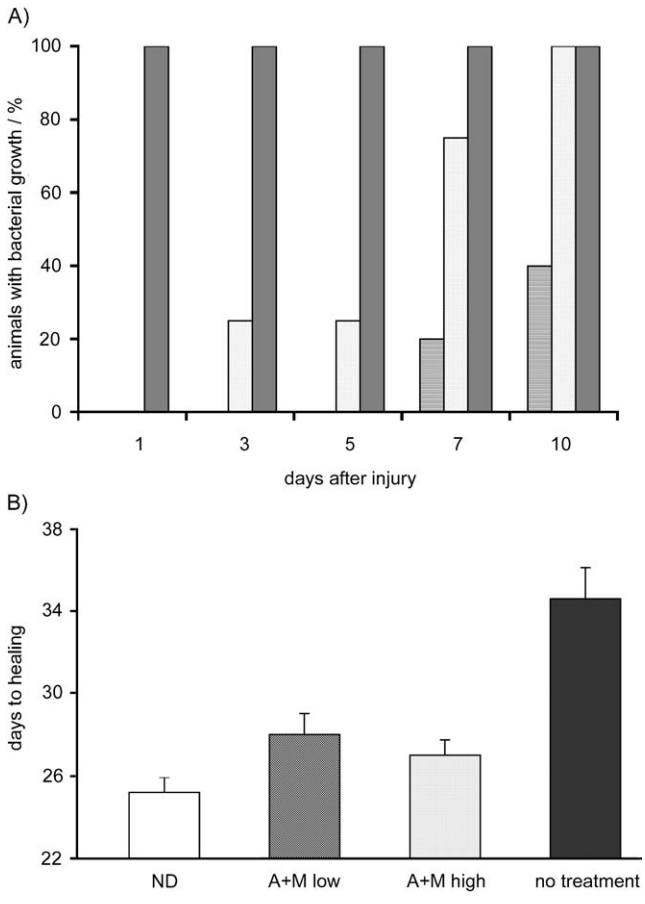

Figure 2. Silver nanoparticles have effective antibacterial properties, but promotion of healing depends on other mechanisms: A) Culture of microorganisms from wound swabs taken on days 1, 3, 5, 7, and 10 in animals treated with ND (light grey), SSD (white) or no treatment (dark grey). B) Time taken for healing of burn wounds in animals treated with ND, antibiotics A + M (amoxicillin + metronidazole at low or high dose), or no treatment.

Silver nanoparticles play a role in cytokine modulation

Because cytokines play an important role in wound healing, we next investigated the expression patterns of IL-6, TGF-β1, IL-10, VEGF, and IFN-γ by using quantitative real-time RT-PCR. Here, levels of IL-6 mRNA in the wound areas treated with silver nanoparticles were maintained at statistically significant lower levels throughout the healing process ($p < 0.01$) (Figure 3 A). mRNA levels of TGF-β1 were higher in the initial period of healing in the ND group; however, this decreased and maintained a lower level during the latter phase of healing ($p < 0.01$) (Figure 3 B). For IL-10, VEGF, and IFN-γ, mRNA levels stayed higher in the ND group relative to those of the SSD group at all time points monitored during healing ($p < 0.01$) (Figures 3 C, D, and E). The differences found in mRNA levels of various cytokines confirm that silver can modulate cytokine expression. In a subsequent experiment, the effects of silver nanoparticles were confirmed to be dose-dependent (data not shown).

Topical delivery of silver nanoparticles suppresses both local and systemic inflammation

To better understand the action of silver nanoparticles on wound healing, we looked at histological sections of the burn wounds from all experimental groups. Although there was an initial influx of neutrophils into the wounds of all experimental groups, we found significantly fewer neutrophils in the ND group on day 7 (Figure 4 A). This suggests a diminished inflammatory response at the wound site.

Furthermore, serum markers of injury were monitored through proteomic analysis. Here we showed that burn injury dramatically stimulated serum expression of hemopexin (Hpx), haptoglobin (Hpg), and serum amyloid protein component P (SAP), all of which are acute-phase proteins. For the first few days after injury, sera from both SSD and ND groups exhibited augmented expression of the acute-phase proteins. The levels of these proteins in the ND group returned to nearly normal levels after day 10. In contrast, the levels in SSD group were still markedly elevated (Figure 4 B).

The effect of silver nanoparticles extends to other wound types

Do silver nanoparticles have the same effect on other wounds? Besides burns, we also investigated wound healing in diabetic mice. In this model, excised wounds treated with silver nanoparticles completely healed in 16 ± 0.41 days after injury, whereas mice in the control group required 18.5 ± 0.65 days ($p < 0.05$). In the nondiabetic littermates, silver nanoparticles still accelerated wound healing relative to the control group (Figure 5).

Discussion

The holy grail for wound healing is accelerated healing without scars. For many years, silver sulfadiazine has been the standard

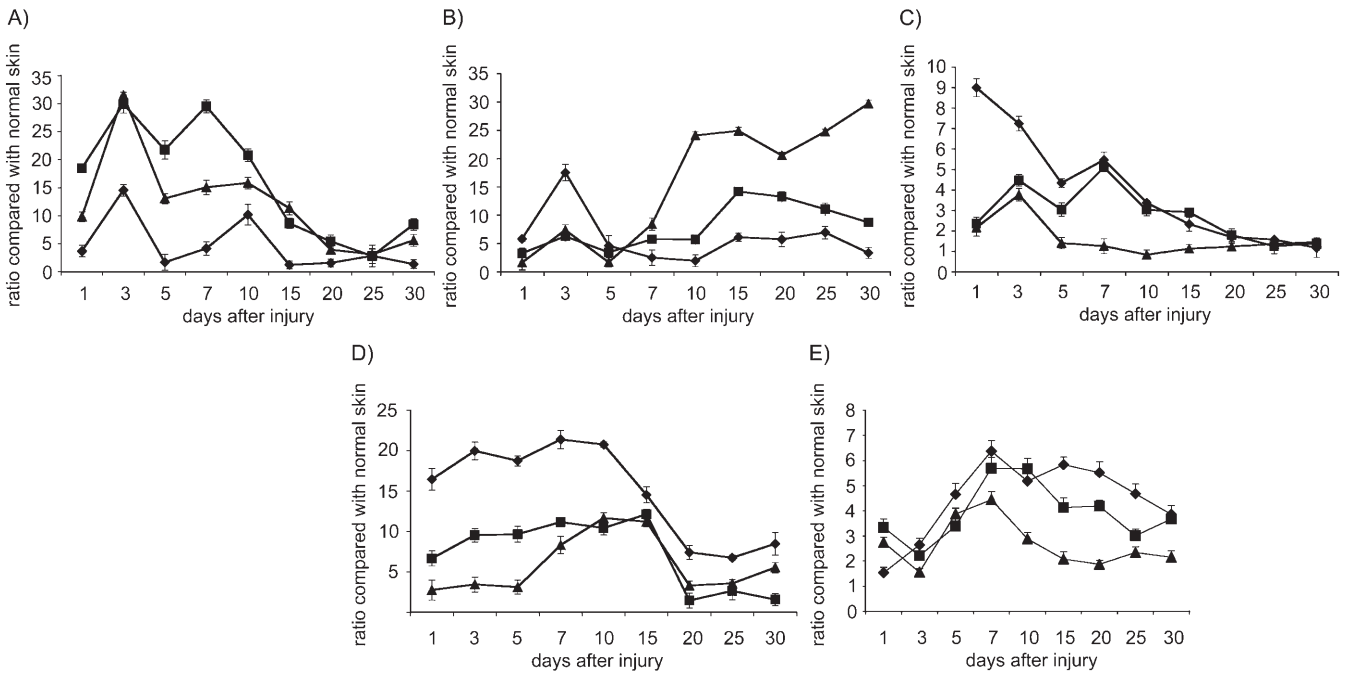

Figure 3. Modulation of cytokine profile by silver nanoparticles: mRNA levels of A) IL-6, B) TGF-β, C) IL-10, D) VEGF, and E) IFN-γ at various time points after burn injury, as determined by quantitative real-time RT-PCR (◆ ND, ▲ SSD, ■ no treatment).

treatment for burns, but some of the benefits of pure silver appear to be lost. Recent advances in nanotechnology have resulted in the ability to produce pure silver as nanoparticles. We therefore hypothesized that silver nanoparticles could improve the healing of burn wounds initially on the basis of the known antimicrobial property of silver. Nonetheless, our findings reported herein not only confirm the efficient antimicrobial property of silver nanoparticles, but also implicate the ability of silver to modulate the cytokines involved in wound healing.

The inflammatory response is an important component of wound healing. Within wounds, various inflammatory mediators are secreted to modulate the healing process. In normal wound healing, the potential for pro- and anti-inflammatory cytokines is certainly present, and the inflammatory response is entirely appropriate. To accomplish successful wound repair and tissue regeneration, the inflammatory response must be tightly regulated in vivo. Among the contributors to delayed wound healing, prolonged inflammatory response is undoubtedly one of the important factors. A vital mediator in this anti-inflammatory cascade appears to be IL-10, which can be produced by keratinocytes as well as inflammatory cells involved in the healing process, including T lymphocytes, macrophages, and B lymphocytes.[26] One of the unique actions of IL-10 is its ability to inhibit the synthesis of pro-inflammatory cytokines, which also include IL-6.[27,28] IL-10 also inhibits leukocyte migration toward the site of inflammation, in part, by inhibiting the synthesis of several chemokines, including monocyte chemoattractant protein-1 (MCP-1) and macrophage inflammatory protein-1α (MIP-1α).[29] Both of the C–C chemokines promote monocyte accumulation, and MIP-1α is also a potent neutrophil chemoattractant in mice.[30] Moreover, studies have shown that MCP-1 and MIP-1α play prominent roles in macrophage recruitment into wounds during wound repair.[31,32]

Within wounds, IL-6 is also secreted by polymorphonuclear cells (PMNs) and fibroblasts. IL-6 has been recognized as an initiator of events in the physiological alterations of inflammation after thermal injury.[33] In fact, an increase in IL-6 concentration parallels the increase in PMN count locally within acute wounds. IL-6 promotes inflammation through monocyte and macrophage chemotaxis and activation.[34] Decreased IL-6 may result in fewer neutrophils and macrophages recruited to the wound and less cytokines being released in the wound with subsequently lower paracrine stimulation of cellular proliferation, fibroblast and keratinocyte migration, and extracellular matrix production. This lack of amplification of the inflammatory cytokine cascade may be important in providing a permissive environment for scarless wound repair to proceed. Silver-induced neutrophil apoptosis and decreased MMP activity may also contribute to the overall decrease in the inflammatory response and as a consequence, an increased rate of wound healing.

In the study reported herein, better cosmetic appearance was observed in animals treated with silver nanoparticles. In terms of wound healing, enhanced expression of TGF-β1 mRNA is found in both keloids and hypertrophic scars. Cumulative evidence has suggested that TGF-β1 plays an important role in tissue fibrosis and post-injury scarring. We showed that lower levels of TGF-β coincided temporally with increased levels of IFN-γ until wound closure in the ND group. As IFN-γ has been demonstrated as a potent antagonist of fibrogenesis through its ability to inhibit fibroblast proliferation and matrix production, its control on TGF-β production may play a role.[35]

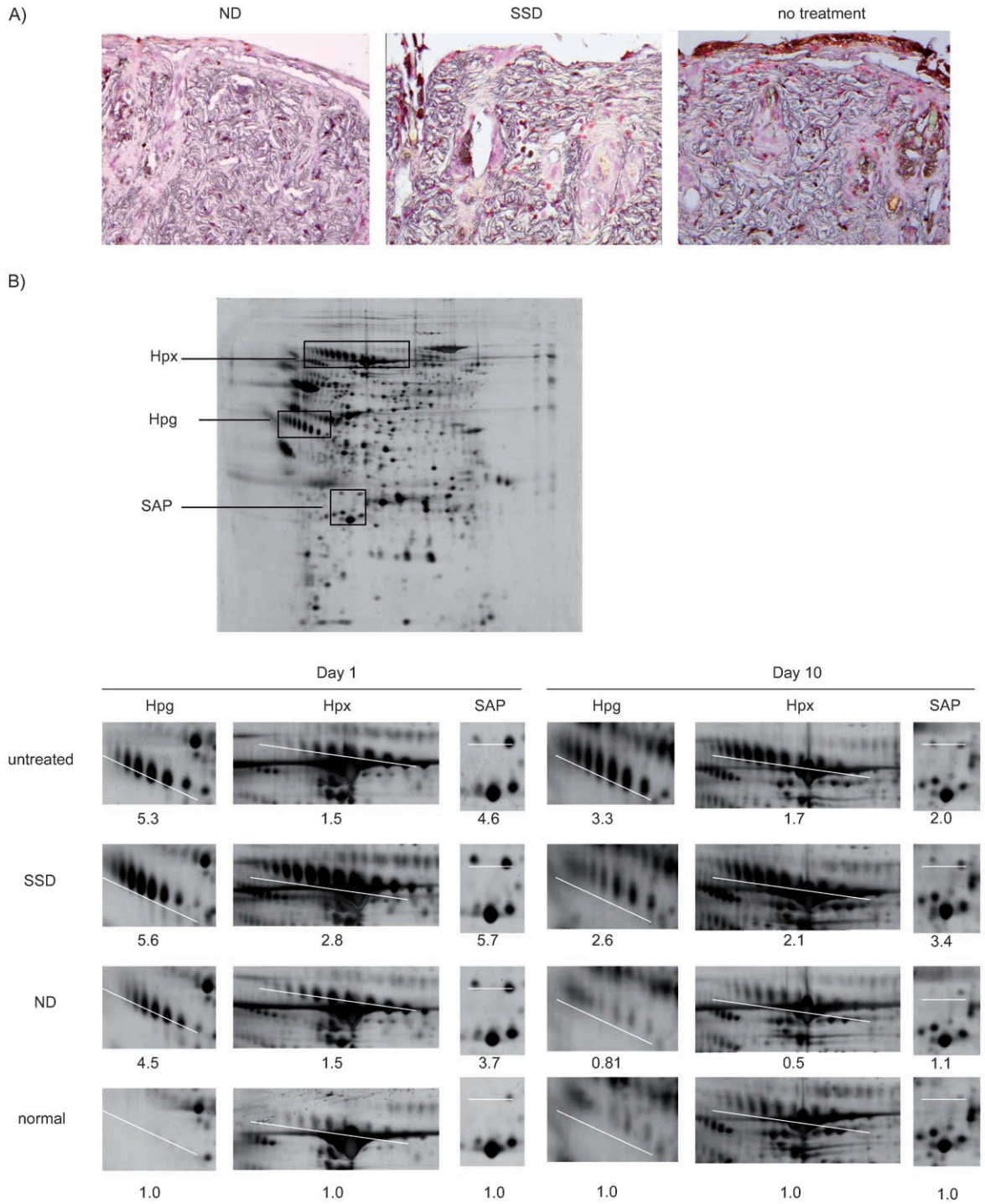

Figure 4. Decreased inflammation at local wound sites and systemically by silver nanoparticles: A) Immunohistochemical staining for neutrophils with naphthol AS-D chloroacetate esterase; comparison between ND, SSD, and no-treatment groups on day 7 after burn injury. Positive staining for neutrophils are denoted by pink spots. B) Monitoring the serum markers of burn injury by proteomic analysis. Sera from mice subjected to burn injury and silver dressing treatment were analysed by 2D gel electrophoresis and MALDI-TOF MS protein identification. Upper panel: Hpx, Hpg, and SAP were identified as serum markers of the burn jury (boxed regions). Lower panel: values below each image reflect the fold change in expression of Hpx, Hpg, and SAP for mice treated with ND, SSD, or control relative to those of normal mice ($n = 5$).

VEGF has been shown to promote healing.[36] Much higher levels of VEGF mRNA are detected in keratinocytes at the wound edge and in keratinocytes that migrate to cover the wound surface. Besides a few mononuclear cells, VEGF expression is not found in other cell types in the wound.[37] This finding suggests that keratinocytes in the wound are a major source of VEGF. As VEGF is highly specific for endothelial cells, it is likely to act in a paracrine manner on the sprouting capil-

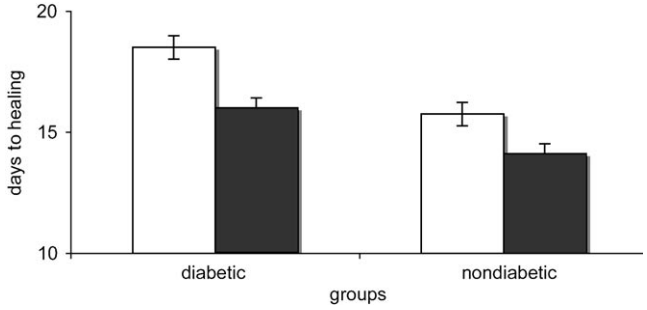

Figure 5. Promotion of diabetic wound healing by silver: time taken for surgically excised wounds to heal in diabetic and control mice using silver nanoparticles (filled bars, $n=5$) or normal saline-treated control group (white bars, $n=5$). Results shown for each group are the mean $\pm$SE of the time required for wound closure. One way ANOVA was used for statistical analysis, and $p<0.05$ was taken as significant.

laries of the wound edge and granulation tissue. Several studies have indicated that TGF-β is able to induce keratinocytes to produce VEGF gene expression.[38,39] From our study, the findings that TGF-β enhanced and reached a peak on day 3 in the ND group may explain why significantly higher VEGF mRNA levels were maintained in the early stage of wound healing.

Taken all these cytokine profiles together, it would appear that an overall decrease in inflammation might be a predicted result in the ND group. Indeed, the reduction of neutrophils observed in histology further confirms this. Corresponding to cytokine and histological analysis, proteomic analysis of the sera of burn-injured mice indicates that Hpx, Hpg, and SAP are major acute-phase proteins induced upon burn injury.[40–43] Hpx and Hpg are plasma glycoproteins that bind heme and hemoglobin, respectively, with high affinity. Their function appears to be to defend against oxidative damage mediated by hemoglobin or free heme that are released into the plasma during intravascular hemolysis upon burn injury. SAP, a member of the pentraxin family of proteins that includes C-reactive protein (CRP), circulates in the blood as a stable pentamer and is ubiquitous in amyloid deposits. In mouse, SAP, rather than CRP, is the major pentraxin acute-phase protein. Our proteomic analysis revealed that the ND group exhibited an earlier normalization of the acute-phase proteins than the SSD group. As hepatic production of Hpx, Hpg, and SAP is known to be stimulated by IL-6, the direct cause of earlier normalization of these acute-phase proteins in the ND group is likely due to the lower levels of IL-6 at the wound sites in this group.

In our study, the overall decrease in the inflammatory response at local wound sites in the ND group mimic the events observed in the PU.1-null mice, further confirming the detrimental effects of inflammation on healing.[17,18] We conclude that silver nanoparticles can modulate local and systemic inflammatory response following burn injury by cytokine modulation. Its use may provide a new and effective therapeutic direction for achieving scarless wound healing in clinical practice.

Experimental Section

Animal experiments

Twenty-week-old male BALB/C mice (Department of Surgery, The University of Hong Kong) weighing between 28 and 32 grams, were used for all thermal injury experiments. *C57BLKs/J-m+/db*, *db/db* (genetically diabetic) and *C57BLKs/J-m* (nondiabetic control) male mice (Jackson Laboratories, USA) were used for the impaired wound-healing animal model. All animals were cared for and procedures were performed in accordance with the University of Hong Kong Committee on the Use of Live Animals in Teaching & Research (animal ethical approval protocol No. CULATR 727-02). For all experiments, mice were anesthetized with an intraperitoneal injection of pentobarbital sodium solution (Abbott Laboratories) at a dose of 60 mg kg^{-1}. Sedation post-procedure was provided for the first 3 days with diazepam (50 mg L^{-1} per day, Roche Pharmaceuticals) added to the drinking water.

A thermal injury animal model has been described previously.[44] Briefly, a burn template was fashioned from a plastic 60-mL syringe by cutting a window (3×2 cm^2) into the side with the opposite half removed so that a mouse could be held horizontally in the burn template. The dorsum of each mouse was carefully shaved from the base of the tail to the base of the neck and laid on the burn template following anaesthesia. The syringe was placed horizontally into a water bath at 70 °C for 35 seconds, followed by immediately placement of the mouse into an iced water bath to stop the burning process. This model would achieve approximately 10% deep partial thickness thermal injury of total body surface area. The mouse was injected with sterile saline intraperitoneally (1 mL) for fluid resuscitation.

For the chronic wound model, *C57BLKs/J-m* and genetically diabetic (*C57BLKs/J-m+/db*, *db/db*) mice were used. The hair on the back of each mouse was shaved, and a piece of full-thickness skin (1×1 cm^2) was excised with scissors.

In both models, the wounds were covered with the appropriate dressings and the animals were bandaged. The dressings were changed daily. During changing of the dressings, wounds were inspected and photographed. Wound swabs were cultured for assessment of microorganism growth. Mice were sacrificed at 1, 3, 5, 7, 10, 15, 20, and 25 days after injury, and the day of wound closure for sample collection. Wound healing is defined as the time at which the wound is completely covered by scab. Five mice were used for each time point for each experimental group.

Tissue samples from scalded wound skin (approximately 3×2 cm^2) of the mice were harvested. Each skin sample was divided for histological analysis and RNA extraction for cytokine evaluation. Blood samples were taken by aortic puncture and immediately transferred into EDTA-coated tubes. After centrifugation at 3000 *g* for 15 min, the serum samples were removed and stored at −70 °C.

All animals were humanely sacrificed by carbon dioxide asphyxiation after the samples were harvested.

Preparation of the dressings

Nanosilver-coated dressing: Initial experiments were carried out by using silver nanoparticle grafted dressing (silver content: 2.75 mg g^{-1}, Anson Nanotechnology Group Co., Ltd. Hong Kong). A piece of silver nanoparticle-coated dressing (4×3 cm^2) weighed 0.1737 g. This corresponds to 0.4777 mg of silver nanoparticles on each piece. Transmission electron microscopy revealed that silver nanoparticles were spherical, with diameters of 14 ± 9.8 nm based on 750 particle measurements on five sites of interest. Subsequent

experiments were performed with silver nanoparticles (1 mM) synthesized by borohydride reduction of $AgNO_3$ in the presence of citrate as a stabilizing agent, as previously described.[45] Similar efficacy with silver nanoparticle dressing was confirmed (data not shown).

SSD dressings: 1% silver sulfadiazine cream $(3.18\ mg\,g)^{-1}$ (Smith & Nephew Pharmaceuticals Ltd.) was used in the control group. SSD (0.1502 g) was applied on a piece of sterile nonadherent absorbent dressing ($4\times3\ cm^2$) to give an equal amount of silver to that of each piece of silver nanoparticle dressing.

Antibiotic dressings: Amoxicillin (A8523, Sigma) and metronidazole (M1547, Sigma) were used in two different concentrations (amoxicillin at 8 and $80\ mg\,L^{-1}$, metronidazole at 1 and $10\ mg\,L^{-1}$). Approximately 3 mL of each solution was dropped on a piece of sterile gauze ($4\times3\ cm^2$) to be used as dressing.

Reverse transcription and real-time polymerase chain reaction (RT-PCR):

Fresh- or snap-frozen skin tissue was homogenized in Trizol (1 mL, Life Technologies) per 50–100 mg of tissue using a homogenizer. RNA was extracted according to the manufacturer's instructions. Total RNA was quantified by optical density at $\lambda = 260$ nm. Complementary DNA (cDNA) was synthesized using TaqMan reverse transcription with MultiScribe reverse transcriptase (Applied Biosystems), according to the manufacturer's protocol. The reaction mixture was exposed to real-time thermal cycling in a PCR system 9700 (Applied Biosystems) with the following conditions: hexamer incubation at 25 °C for 10 min, reverse transcription at 37 °C for 60 min, and the temperature was raised to 95 °C for 5 min to stop the reaction. After thermal cycling, the final cDNA product was stored at −20 °C for subsequent cDNA amplification by PCR.

PCR mixtures (final volume: 25 μL) contained TaqMan cytokine gene expression reagents (Applied Biosystems) with cytokine-specific target primers and fluorogenic probe (IL-10, Mm00439616_m1; IL-6, Mm00446190_m1; TGF-β1, Mm00441724_m1; VEGF, Mm00437304_m1, SIG1020000, 1020300000; and IFN-γ, Mm00801778_m1; FAM dye layer, Applied Biosystems), endogenous reference primers, and probe (rRNA, VIC dye layer) in MicroAmp optical 96-well reaction plates with optical caps. PCR reactions were performed in a Gene-Amp PCR system 9600 (Applied Biosystems). Each PCR amplification was performed by using the following conditions: 2 min at 50 °C and 10 min at 95 °C, followed by a total of 40 or 45 two-temperature cycles (15 s at 95 °C and 1 min at 60 °C). The FAM dye layer yields the results for quantitation of the cytokine target mRNA, while the VIC dye layer yields the results for quantitation of the 18S ribosomal RNA endogenous control. In all experiments, controls without template as well as control RNA (Applied Biosystems) were included.

The relative quantitation values for the cytokine gene-expression assays were calculated from the accurate C_T value according to the manufacturer's description (protocol P/N 4303859, PerkinElmer). The C_T value for rRNA (VIC) was subtracted from the specific cytokine C_T value (FAM for IL-10, IL-6, TGF-β1, IFN-γ and VEGF) to calculate ΔC_T for the calibrator (normal skin) and samples (wounds) in each cytokine gene-expression assay. ΔC_T values for triplicate wells of the calibrator (normal skin) for each cytokine were averaged.

Histological techniques and immunohistochemistry:

Wound skin was cut into strips (5–10 mm) and placed in neutralized formalin (10%, HT50–1–128, Sigma–Aldrich) overnight. Wound strips were paraffin-embedded for cross-sectioning at (thickness: 6 μm) before staining with hematoxylin and eosin.

For neutrophil staining, the naphthol AS-D chloroacetate esterase procedure (Sigma 91C kit) was used. Briefly, a solution of sodium nitrite (1 mL) and a solution of fast red violet LB vase (1 mL) were mixed gently by inversion and allowed to stand for 2 min. The mixed solution was added to pre-warmed deionized water (40 mL). Then trizmal 6.3 buffer concentrate (5 mL) was added, followed by a solution of naphthol AS-D chloroacetate (1 mL). The slides were incubated for 15 min at 37 °C, and were then rinsed thoroughly in deionized water. A solution of hematoxylin was used to counterstain for 2 min.

Proteomic analysis of serum makers of thermal injury: Mouse sera were subjected to 2D gel electrophoresis and MALDI-TOF MS. A serum volume of 2 μL was run on IPGphor IEF and electrophoresis system (GE Health Care) according to the manufacturer's instructions. The resolved proteins were visualized by silver staining, and the gels were scanned with an ImageScanner (GE Health Care). Protein spots on the image files were quantified with ImageMaster 2D Elite software (GE Health Care), and those with consistent differences between samples were cut out. After in-gel tryptic digestion, the resulting peptides were identified by MALDI-TOF MS. MS spectra were recorded using a MALDI-TOF mass spectrometer (Voyager-DE STR, Applied Biosystems). NCBI database searching was manually performed using the MS-Fit program (http://prospector.ucsf.edu) with a mass tolerance setting of 50 ppm.

Statistical analysis: Statistical differences were determined using *t* test and ANOVA. A p value of < 0.05 was taken as statistically significant.

Keywords: cytokines · medicinal chemistry · nanostructures · proteomics · silver · wound healing

[1] P. Martin, *Science* **1997**, *276*, 75–81.
[2] M. H. Branton, J. B. Kopp, *Microbes Infect.* **1999**, *1*, 1349–1365.
[3] S. M. Wahl, *Microbes Infect.* **1999**, *1*, 1247–1249.
[4] A. Ghahary, Y. J. Shen, P. G. Scott, Y. Gong, E. E. Tredget, *J. Lab. Clin. Med.* **1993**, *122*, 465–473.
[5] L. L. Hsiao, S. Jaakkola, S. Sollberg, M. Aumailley, R. Timpl, M. L. Chu, J. Uitto, *J. Invest. Dermatol.* **1991**, *97*, 240–248.
[6] D. J. Whitby, M. W. Ferguson, *Dev. Biol.* **1991**, *147*, 207–215.
[7] S. M. Wahl, J. B. Allen, G. L. Costa, H. L. Wong, J. R. Dasch, *J. Exp. Med.* **1993**, *177*, 225–230.
[8] M. Shah, D. M. Foreman, M. W. Ferguson, *J. Cell Sci.* **1995**, *108*, 985–1002.
[9] R. B. Mateo, J. S. Reichner, J. E. Albina, *Am. J. Physiol.* **1994**, *266*, R1840–R1844.
[10] K. W. Liechty, N. S. Adzick, T. M. Crombleholme, *Cytokine* **2000**, *12*, 671–676.
[11] M. J. Dans, R. Isseroff, *J. Invest. Dermatol.* **1994**, *102*, 118–121.
[12] K. Tamai, H. Ishikawa, A. Mauviel, J. Uitto, *J. Invest. Dermatol.* **1995**, *104*, 384–390.
[13] E. E. Tredget, R. Wang, Q. Shen, P. G. Scott, A. Ghahary, *J. Interferon Cytokine Res.* **2000**, *20*, 143–151.
[14] B. J. Broker, D. Rosen, J. Amsberry, R. Schmidt, L. Sailor, E. A. Pribitkin, W. M. Keane, *Laryngoscope* **1996**, *106*, 1497–1501.
[15] Y. Sato, T. Ohshima, T. Kondo, *Biochem. Biophys. Res. Commun.* **1999**, *265*, 194–199.
[16] K. W. Liechty, H. B. Kim, N. S. Adzick, T. M. Crombleholme, *J. Pediatr. Surg.* **2000**, *35*, 866–872.
[17] P. Martin, D. D'Souza, J. Martin, R. Grose, L. Cooper, R. Maki, S. R. McKercher, *Curr. Biol.* **2003**, *13*, 1122–1128.
[18] L. Cooper, C. Johnson, F. Burslem, P. Martin, *Adv. Genome Biol.* **2005**, *6*, R5.
[19] H. J. Klasen, *Burns* **2000**, *26*, 131–138.
[20] J. Hanif, R. A. Tasca, A. Frosh, K. Ghufoor, R. Stirling, *Clin. Otolaryngol. Allied Sci.* **2003**, *28*, 368–370.

[21] L. Antonangelo, F. S. Vargas, L. R. Teixeira, M. M. Acencio, M. A. Vaz, M. T. Filho, E. Marchi, *Lung* **2006**, *184*, 105 – 111.
[22] S. M. Modak, C. L. Fox, Jr., *Biochem. Pharmacol.* **1973**, *22*, 2391 – 2404.
[23] J. B. Wright, K. Lam, A. G. Buret, M. E. Olson, R. E. Burrell, *Wound Repair Regen.* **2002**, *10*, 141 – 151.
[24] F. R. Fan, A. J. Bard, *Proc. Natl. Acad. Sci. USA* **1999**, *96*, 14222 – 14227.
[25] R. W. Sun, R. Chen, N. P. Chung, C. M. Ho, C. L. Lin, C. M. Che, *Chem. Commun.* **2005**, *40*, 5059 – 5061.
[26] K. W. Moore, A. O'Garra, R. de Waal Malefyt, P. Vieira, T. R. Mosmann, *Annu. Rev. Immunol.* **1993**, *11*, 165 – 190.
[27] D. F. Fiorentino, A. Zlotnik, P. Vieira, T. R. Mosmann, M. Howard, K. W. Moore, A. O'Garra, *J. Immunol.* **1991**, *146*, 3444 – 3451.
[28] R. de Waal Malefyt, J. Abrams, B. Bennett, C. G. Figdor, J. E. de Vries, *J. Exp. Med.* **1991**, *174*, 1209 – 1220.
[29] M. N. Ajuebor, A. M. Das, L. Virag, C. Szabo, M. Perretti, *Biochem. Biophys. Res. Commun.* **1999**, *255*, 279 – 282.
[30] R. Alam, D. Kumar, D. Anderson-Walters, P. A. Forsythe, *J. Immunol.* **1994**, *152*, 1298 – 1303.
[31] L. A. DiPietro, *Shock* **1995**, *4*, 233 – 240.
[32] E. Engelhardt, A. Toksoy, M. Goebeler, S. Debus, E. B. Brocker, R. Gillitzer, *Am. J. Pathol.* **1998**, *153*, 1849 – 1860.
[33] P. Paquet, G. E. Pierard, *Int. Arch. Allergy Immunol.* **1996**, *109*, 308 – 317.
[34] P. Biswas, F. Delfanti, S. Bernasconi, M. Mengozzi, M. Cota, N. Polentarutti, A. Mantovani, A. Lazzarin, S. Sozzani, G. Poli, *Blood* **1998**, *91*, 258 – 265.
[35] M. R. Duncan, B. Berman, *J. Exp. Med.* **1985**, *162*, 516 – 527.
[36] M. Artuc, B. Hermes, U. M. Steckelings, A. Grutzkau, B. M. Henz, *Exp. Dermatol.* **1999**, *8*, 1 – 16.
[37] L. F. Brown, K. T. Yeo, B. Berse, T. K. Yeo, D. R. Senger, H. F. Dvorak, L. van de Water, *J. Exp. Med.* **1992**, *176*, 1375 – 1379.
[38] M. Momose, M. Murata, Y. Kato, K. Okuda, K. Yamazaki, C. Shinohara, H. Yoshie, *J. Periodontol.* **2002**, *73*, 748 – 753.
[39] D. Beddy, R. W. Watson, J. M. Fitzpatrick, P. R. O'Connell, *Br. J. Surg.* **2004**, *91*, 72 – 77.
[40] E. Tolosano, F. Altruda, *DNA Cell Biol.* **2002**, *21*, 297 – 306.
[41] S. Gordon, *Curr. Biol.* **2001**, *11*, R399 – 401.
[42] C. J. de Haas, *FEMS Immunol. Med. Microbiol.* **1999**, *26*, 197 – 202.
[43] K. Zahedi, A. S. Whitehead, *J. Immunol.* **1989**, *143*, 2880 – 2886.
[44] R. K. Cribbs, M. H. Luquette, G. E. Besner, *J. Surg. Res.* **1998**, *80*, 69 – 74.
[45] R. Jin, Y. Cao, C. A. Mirkin, K. L. Kelly, G. C. Schatz, J. G. Zheng, *Science* **2001**, *294*, 1901 – 1903.

Received: September 22, 2006
Published online on October 31, 2006

